applied sciences

MDPI

Article

Automatic Transmission Fluids in Electrified Transmissions: Compatibility with Elastomers

Alejandro García-Tuero [1], Beatriz Ramajo [2], Guillermo D. Valbuena [1], Alfonso Fernández-González [3], Rafael Mendoza [2], Alberto García [1,*] and Antolin Hernández Battez [1]

[1] Department of Construction and Manufacturing Engineering, University of Oviedo, 33204 Gijón, Spain; garciatalejandro@uniovi.es (A.G.-T.); guille.d.valbuena@gmail.com (G.D.V.); aehernandez@uniovi.es (A.H.B.)
[2] Scientific and Technical Services, University of Oviedo, 33006 Oviedo, Spain; ramajobeatriz@uniovi.es (B.R.); rafam80@gmail.com (R.M.)
[3] Department of Physical and Analytical Chemistry, University of Oviedo, 33006 Oviedo, Spain; fernandezgalfonso@uniovi.es
* Correspondence: garciamaralberto@uniovi.es; Tel.: +34-985-18-1925

Featured Application: Electric vehicle transmission.

Abstract: The location of the electric motor (EM) inside the transmission in an electric vehicle requires the compatibility of the automatic transmission fluids (ATFs) with the materials of the EM and the transmission. This work studies the compatibility of four conventional ATFs with three elastomers: fluoroelastomer (FKM), ethylene-propylene-diene monomer (EPDM), and vinyl-methyl silicone rubber (silicone). Changes in volume, hardness, tensile strength, and elongation at break of the elastomers after aging in the ATFs were measured, and additional Fourier transform infrared spectroscopy (FTIR), X-ray diffraction (XRD), and thermogravimetric and derivative thermogravimetric (TGA and DTGA) tests were performed. The four ATFs showed high or medium compatibility with FKM and silicone, and low compatibility with EPDM. This low compatibility was related to changes in the composition and crystalline structure of the elastomer. The non-compatibility of the EPDM with the oils from Group III was also proven.

Keywords: electric vehicle; automatic transmission fluids; materials compatibility; elastomers

Citation: García-Tuero, A.; Ramajo, B.; Valbuena, G.D.; Fernández-González, A.; Mendoza, R.; García, A.; Hernández Battez, A. Automatic Transmission Fluids in Electrified Transmissions: Compatibility with Elastomers. *Appl. Sci.* **2022**, *12*, 6213. https://doi.org/10.3390/app12126213

Academic Editors: Alessandro Ruggiero and Ramin Rahmani

Received: 20 May 2022
Accepted: 16 June 2022
Published: 18 June 2022

1. Introduction

The electric vehicle (EV) has been adopted by governments as one of the main solutions in the struggle to minimise transportation-related emissions which, according to the Intergovernmental Panel on Climate Change [1], represent 14% of emitted global greenhouse gasses. The average efficiency of the EV is 77%, which is a great improvement when compared to the 21% of the traditional internal combustion engine (ICE) vehicle [2]. The energetic efficiency results in big reductions in CO_2 emissions [3], an effect which is even greater when the electricity used is generated from renewable sources [4]. There are many types of EVs, from full electric vehicles such as extended range electric vehicles (EREV) or battery electric vehicles (BEV), to hybrid electric vehicles (HEV) or plug-in hybrid electric vehicles (PHEV), and mild hybrid electric vehicles (MHEV) or fuel cell electric vehicles (FCEV). Moreover, independently of the EV type, the position of the electric motor (EM) can be before, after or inside the transmission of the vehicle [5], or even directly next to the wheels [6]. When the EM is located inside the transmission, it is in contact with the transmission fluid, a circumstance that may occur both in hybrid vehicles and in 100% electric vehicles, which require a transmission to adapt the speed of the motor to the speed required at the wheels of the vehicle. For that reason, the requirements of automatic transmission fluids (ATFs) are more demanding than in ICE vehicles. Among these requirements are magnetic, thermal, electrical and materials compatibilities [6–8].

The growing importance of EVs in the context of reducing global emissions makes it of especial interest to analyse the interaction between EV transmission lubricants and the materials used in them. The compatibility of the lubricants with seal materials that are commonly found in transmissions is tested by evaluating the variation in volume, hardness, tensile strength, and elongation at break after aging in the ATF (for 168 h) [9,10]. This is the case of several elastomers that are frequently used in seals, gaskets, and the insulation of electrical wires [11], such as ethylene-propylene-diene monomer (EPDM), fluoroelastomer (FKM), or vinyl-methyl silicone rubber (silicone). The swelling and degradation of elastomers caused by some oils have been previously reported by other authors [12,13], as the physical properties of these materials need to remain stable in order to prevent oil leakages.

This research has the objective of studying the compatibility of four commercial ATFs with certain elastomers commonly used in electrified transmissions as seals, gaskets, and electrical insulators. Measurements of volume, hardness, tensile strength, and elongation at break were made for three elastomers (EPDM, silicone, and FKM), following the international standards recommendations [14]. The tested materials were aged in the four ATFs for the time recommended by different specifications or standards (168 h) and, in addition, for longer time periods (336, 504, and 672 h). To explain the changes that occurred in the properties of the elastomers, additional tests such as Fourier transform infrared spectroscopy (FTIR), X-ray diffraction (XRD), and thermogravimetric and derivative thermogravimetric analysis (TGA and DTGA) were performed on the elastomers.

The novelty of this research consists of studying the materials compatibility of four ATFs with different compositions at longer aging times than that recommended by the corresponding standards. This compatibility study is a part of a broader research project, whose goal is the formulation of appropriate lubricants for electric vehicles and where other compatibility tests (electrical, thermal, copper corrosion by wire resistance, etc.) will be performed.

2. Materials and Methods

2.1. Materials

The compatibility of four commercial ATFs with three elastomeric materials was studied. Both the ATFs and elastomers are commonly used by car manufacturers at the time of writing. Table 1 shows the base oils which are composed each ATF and their concentration, as well as some physicochemical properties of the ATFs.

Table 1. Properties of the ATFs.

ATF	Base Oils (wt.%)	Density (kg/m^3)	Kin. Viscosity (cSt) [1]		VI [2]
		15 °C	100 °C	40 °C	
Oil A	Group I, 4.9 cSt/100 °C (77.7) Group I, 2.7 cSt/100 °C (10.6)	869	7.8	43	161
Oil B	Group III, 3.0 cSt/100 °C (38.3) Group III, 6.5 cSt/100 °C (50.7)	847	6	30	151
Oil C	Group III, 3.0 cSt/100 °C (45.0) Group III, 6.5 cSt/100 °C (38.5)	854	7.2	35	181
Oil D	Group III, 3.0 cSt/100 °C (36.5) Group III, 4.2 cSt/100 °C (36.5)	854	6.9	34	165

[1] 1 [cSt] = 1×10^{-6} [m^2/s]; [2] Viscosity index (VI).

The four ATFs are each composed of two base oils, which may vary from one to another, and an additive package which is also different for each ATF (Table 1). Oil A is composed of a mixture of two base oils from Group I and 11.7 wt.% of additives. Oils B, C, and D are composed of mixtures of two base oils from Group III and an additive content of 11, 17, and 27 wt.%, respectively.

Table 2 shows the main properties of the studied elastomers. These elastomers (FKM, silicone, and EPDM) are commonly used as seals and gaskets in transmissions and also as insulator of electrical wires [15]. Although the EPDM is considered as non-compatible with mineral oils, it was included in this study in order to determine if the base oils from Group III, also considered as synthetics, are compatible with this material [16]. Table 2 shows the main characteristics of the elastomers as given by the provider. The specimens for measurements of mechanical properties were prepared with the dimensions specified (type V) in the ASTM D638 standard and were extracted from sheets of each material.

Table 2. Properties of the elastomers.

	FKM [1]	EPDM [2]	Silicone [3]
Density (kg/m^3)	-	1130	1300
Tensile Strength (MPa)	9.8	12	5
Elongation at break (%)	165	360	450
Hardness (Shore A)	70	70	60
Max. op. temperature (°C)	204	100	200

[1] Fluorocarbon (FKM); [2] Ethylene propylene diene monomer (EPDM); and [3] Vinyl-methyl silicone rubber (silicone).

2.2. Aging Process of the Different Materials

The specimens were wiped carefully with a moist cloth to eliminate any machining debris that could be present. After that, they were soaked in ethanol and dried with hot air and blotting paper.

The aging procedure followed the ASTM D7216-15 standard [14]. A MEMMERT Universal Oven (Model U, precision: ±0.5 °C) kept the temperature constant at 100 °C while the specimens were separately immersed in the ATFs for one week (168 h). Furthermore, it was decided to continue the aging procedure of the elastomers for two (336 h), three (504 h), and four (672 h) weeks in order to verify the long-term behaviour of the different 'ATF/elastomer' combinations.

Once the specimens were extracted from the oven, they were dried with blotting paper to eliminate oil. The cleaning process was completed by rinsing the specimens in ethanol and drying in hot air.

2.3. Materials Characterization

The ASTM-D7216 standard was used to evaluate the compatibility of the four ATFs and the three elastomers by measuring the changes in the elastomers with respect to volume, hardness, and tensile strength after having been aged in the oils.

Changes in volume were measured with a Radwag AS 310.R2 Analytical Balance (readability: 0.1 mg). A recipient with water was weighed before and after the specimens were dipped in it, suspended from a copper thread. The specimen displaced an equal volume of water, which was calculated by the difference in weight. The hardness of the elastomers was measured with a SAUTER HBA 100 durometer. The reference hardness was measured on three fresh specimens, while the hardness of the aged specimens was measured at four different points for each specimen, and the mean value used. An MTS© Sinergy traction machine, which has a charge cell of 5 kN (MTS-166), was used to measure the tensile strength. The setting was based on the material and aging time, according to ASTM D638 recommendations, to keep the testing time under 5 min. Table 3 shows the traction speed used for each material and each aging time.

2.4. Complementary Tests

X-ray diffraction (XRD) data were collected at room temperature using CuKα1,2 radiation (λ = 1.54056 Å and 1.54439 Å) in a Bragg–Brentano reflection configuration on a PHILIPS X' PERT PRO Panalytical diffractometer in a 2θ range of 6–70°. The step size was 0.0167°.

A Varian 670-IR FTIR spectrometer with a Golden Gate ATR device was used to implement Fourier transformed infrared spectroscopy (FTIR) tests on the elastomers. The results showed variations in the composition of the materials after the aging process. The resolution range of the spectrometer was from 4 to 2000 cm^{-1}. Each specimen was scanned 16 times.

Table 3. Traction speed (in m/s) by material and aging time.

Aging Time (h)	FKM	EPDM	Silicone
168	0.020	0.025	0.025
336	0.015	0.025	0.030
504	0.015	0.025	0.030
672	0.015	0.025	0.030

Thermal characterization of the samples was carried out by thermogravimetric analysis in an SDT Q600 thermal analyser (TA Instruments). A nitrogen atmosphere (gas flow rate of 100 cm^3/min) was used to remove all gases formed in the heating process and to avoid further thermo-oxidative degradation. The samples were cut into cubes and weighed between 20 and 25 mg. They were heated from room temperature to 800 °C at a 10 °C/min heating rate. The loss of weight, the initial and terminal degradation temperatures (T_{onset} and T_{endset}), and the peak temperature for the maximum loss of mass (T_{max}) were determined using the Universal analysis 2000 software package, supplied with the thermal analyser.

3. Results and Discussion

Numerous specifications determined by transmission manufacturers establish permissible limits for changes in the properties of the elastomeric materials in contact with the ATFs [9]. The allowed changes in volume and hardness of the elastomers used in the transmission are specified in the Ford, Ford Mercon V, Allison Transmission, Allison TES 439, GM, and Dexron VI specifications. In the case of the tensile strength and the elongation at break, only Allison TES 439 and Allison TES 389 (Rev. B) give limit values for the elastomer response after aging in ATFs.

3.1. Changes in Volume

Figure 1 shows the volume variations expressed as the ratio of the volume variation to the initial volume (as a percentage). Negative values indicate a reduction in volume after aging, while positive values indicate an increase in volume. The compatibility of the elastomers with the ATFs regarding volume change was initially tested after 168 h, as specified in standard ASTM D7216-15 [14], but effects of longer aging times are also reported in Figure 1. The dashed horizontal black lines indicate the range of volume variation accepted for each material by the manufacturer's specifications [9]. In the case of FKM, these dashed lines indicate the maximum swelling and shrinking accepted. For silicone, the upper line indicates the maximum accepted variation, and the lower line indicates the maximum recommended limit. In EPDM, there are no recommended values in the literature, so there are no acceptance values indicated in the figure. Silicone showed a volume variation lower than the maximum limit values recommended by the transmissions manufacturers [9]. On the other hand, the FKM constitutes a special case, as the volume of the specimens was reduced their after aging whereas, according to the results in Drobny [17], they were expected to swell. Although the Allison TES 439 specification [9] accepts up to a 2% volume decrease for this material, the FKM samples shrank between 2.5 and 3.5%, which is out of specification. The EPDM underwent a considerable increase in volume, the maximum values being obtained with oil A. Although no volume change specification exists for this elastomer, the values here reported lead to the conclusion that these oils are not compatible with this material.

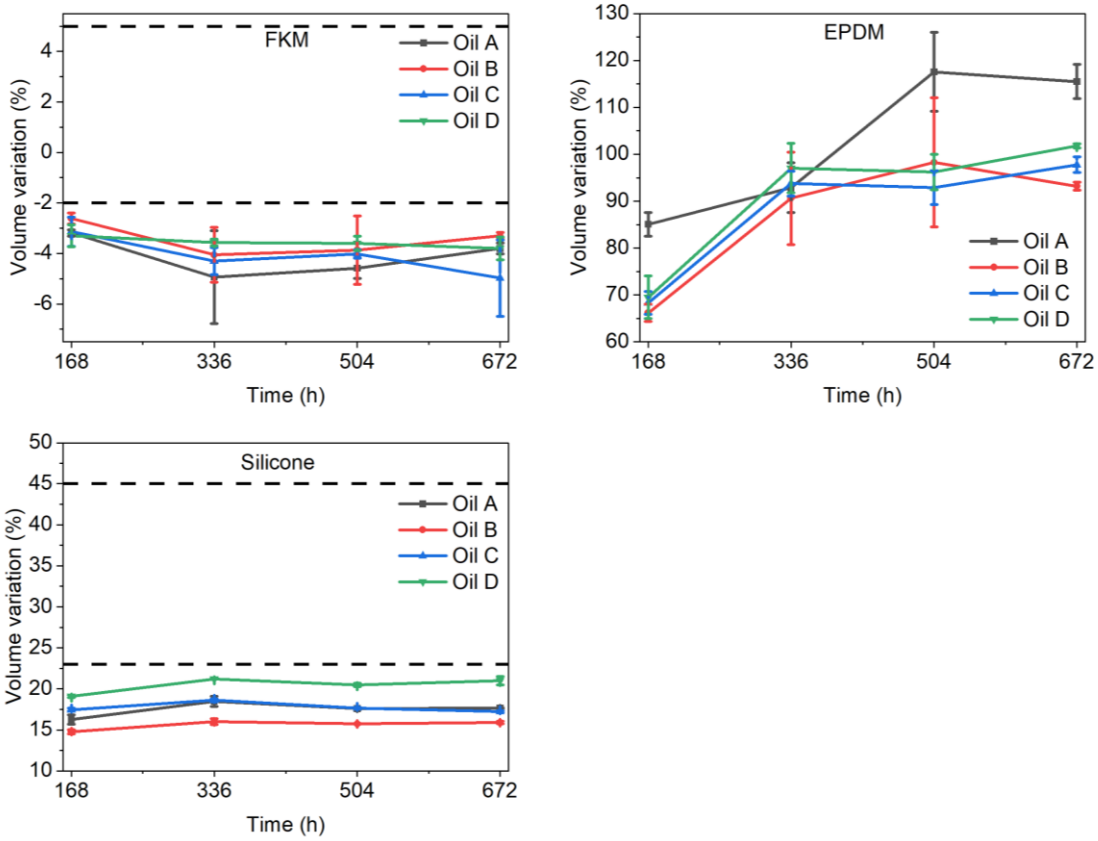

Figure 1. Changes in volume (expressed as the ratio of the volume variation to the initial volume) of the FKM, silicone, and EPDM after aging in oils A, B, C, and D.

Regarding the long-term evolution of the volume variation (from 168 h onwards), the silicone samples hardly changed during the entire period of aging, with volume variations of around ±1%. The EPDM increased in volume after aging in all of the ATFs used from 168 h onwards. However, it remained nearly constant after 336 h in oils B, C, and D. The highest volume change values were caused by oil A. EPDM increased in volume in this oil up to an aging time of 504 h, but after that time, it remained constant until the end of the test. The FKM showed a reduction in volume in all the ATFs, with values nearly constant after 336 h and outside all the specifications (Allison TES 439 has the lowest admissible volume change limit: −2%). So, the tested oils are not compatible with FKM in terms of volume change. Considering the available specifications for the volume changes of elastomers aged in ATFs, it could be concluded that only the silicone fulfils the volume change requirements.

3.2. Changes in Hardness

The abovementioned specifications were also used to analyse the compatibility of the materials regarding changes in hardness. Figure 2 shows the evolution in hardness of the different elastomers during the aging process expressed in Shore A scale. Acceptation limits values from manufacturers are not indicated in the figure as these limits are not absolute values but are also given related to initial hardness of the material [9]. While the FKM showed small changes in hardness in the first 168 h, the EPDM and silicone showed a huge reduction, but within the limits allowed by transmissions manufacturers in the case of the silicone. Kusuhara et al. [18] reported a similar drop in hardness for silicone, around 15 points (Shore A), after only 72 h of aging in engine oil, with a variety of additives and at 150 °C. There is no bibliographical reference to the behaviour of EPDM in oils, but its loss of hardness is by far the greatest of the three elastomers. Nakamura et al. [19] reported a large reduction in hardness for EPDM seals after they were used in a water supply system

for three years at temperatures between 20 and 45 °C. It seems to be the immersion in fluids that affects the hardness of the EPDM, as de Souza reported no hardness reduction after 360 h of thermo-oxidative aging at 120 °C [20]. The changes in hardness of each elastomer after aging in oils were not greatly affected by the oil used. Regarding the FKM, Drobny [17] reported negligible hardness changes after one week of aging at 150 °C in engine and wheel-bearing oils, and null at 250 °C without aging, confirming the results shown in Figure 2.

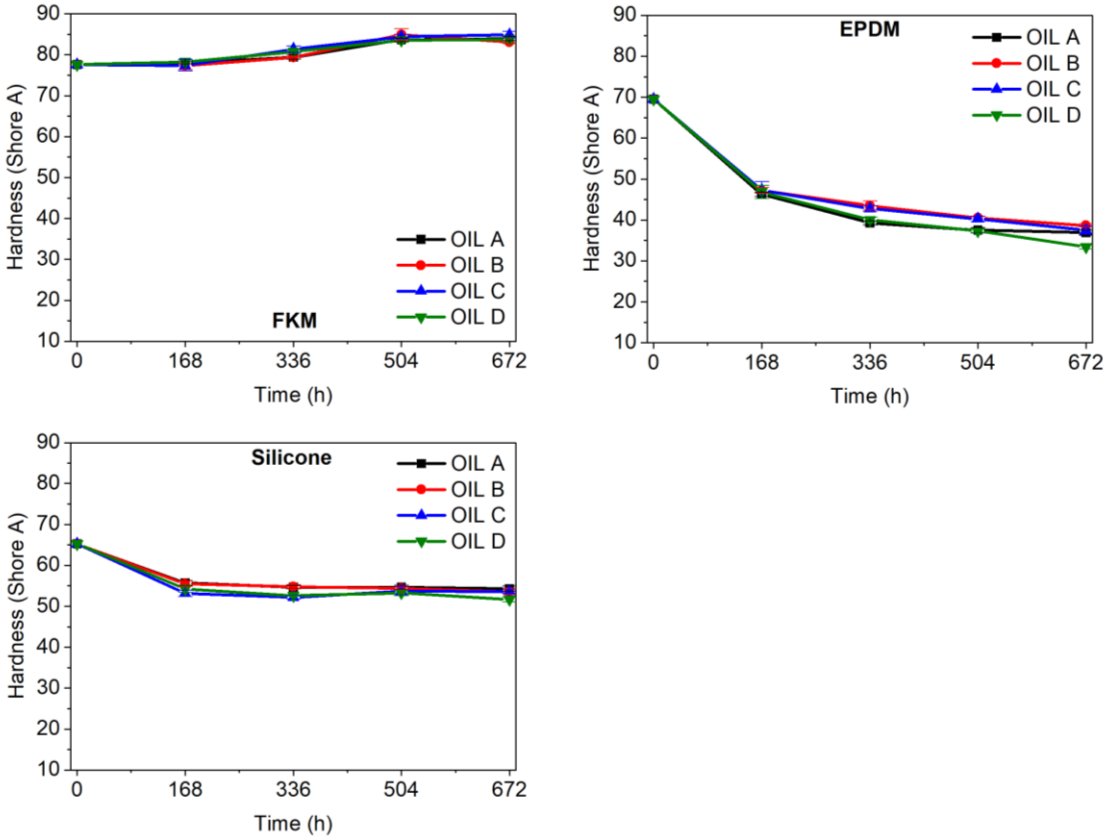

Figure 2. Changes in hardness of the FKM, EPDM, and silicone after aging in oils A, B, C, and D.

From 168 h onwards, the silicone showed insignificant variation in hardness, but that was not the case for the EPDM and the FKM. The EPDM had a greater loss of hardness but there is no specification for this material regarding hardness change. While the EPDM showed a continuous reduction in hardness, that of FKM increased. Taking into consideration the specifications from manufacturers, the silicone fulfilled all the requirements respecting admissible changes in hardness, Ford's being the most restrictive (−30 ShA). This material showed a lower decrease in hardness when aged (672 h) at room temperature [21]. It was the high temperature, rather than the oil type, that led to a decrease in the hardness of the silicone.

In the case of the FKM, its hardness variation exceeds the Ford, Allison Transmission, and Dexron VI specifications (+5 ShA) after 336 h for oils A, B, and C, and also after 504 h for oil D. The FKM also exceeds the GM specifications (+6 ShA) for oils A, B, and C after 504 h, and for oil D after 672 h. In addition, the FKM exceeds the Allison TES 439 specifications (+7 ShA) for oil B after 504 h and for oil C after 672 h. On the contrary, the FKM fulfilled the Ford Mercon V specifications (limit value: −8 ShA points) during the whole test and for all the oils tested. The results in Petit et al. [22] confirm what is shown in Figure 2, as they obtained a slight hardening of FKM after prolonged aging in lubricants at 150 °C.

3.3. Changes in Tensile Strength and Elongation at Break

Table 4 shows the values of tensile strength of all the aged elastomers as well as the fresh samples (0 h aging). These values of Table 4 allow us to analyse and compare the absolute tensile strength of all studied elastomers. Figures 3 and 4 show the percentage variation in the tensile strength and the elongation at break of the different materials after the aging process and allows us to analyse the relative evolution of these characteristics. The values of the fresh material are taken as a reference to establish the percentage variation. Horizontal discontinuous black lines indicate the acceptance variations reported in the literature for the FKM and silicone (upper and lower limits) [9]. EPDM acceptance limits are not reported in the literature.

Table 4. Tensile strength (MPa) and standard deviation (in brackets) for the different elastomers and different aging times and ATFs.

ATF	Aging (h)	FKM	EPDM	Silicone
Fresh	0	10.57 (1.62)	9.57 (0.31)	10.03 (0.47)
Oil A	168	10.40 (0.26)	3.00 (0.20)	7.23 (1.34)
	336	8.73 (0.40)	2.87 (0.15)	7.67 (0.29)
	504	9.33 (0.96)	2.37 (0.21)	6.63 (0.55)
	672	9.55 (0.07)	2.57 (0.21)	6.97 (0.50)
Oil B	168	9.43 (0.49)	9.57 (0.31)	7.53 (0.57)
	336	6.83 (0.21)	3.43 (0.32)	6.83 (0.45)
	504	7.13 (0.12)	2.73 (0.31)	7.43 (0.12)
	672	7.47 (0.25)	3.33 (0.25)	7.30 (0.20)
Oil C	168	10.37 (0.38)	2.97 (0.38)	4.07 (0.23)
	336	7.93 (0.21)	9.57 (0.31)	2.83 (0.12)
	504	8.27 (0.85)	4.23 (0.76)	2.47 (0.15)
	672	8.20 (0.36)	3.03 (0.21)	2.10 (0.10)
Oil D	168	9.87 (0.38)	2.77 (0.21)	10.03 (0.47)
	336	7.13 (0.32)	2.83 (0.25)	6.67 (0.58)
	504	7.80 (0.36)	9.57 (0.31)	6.00 (0.46)
	672	7.80 (0.17)	3.17 (0.29)	5.87 (0.49)

The complete stress–strain curves of the three elastomers (fresh and aged) for different periods of time are reported in Supplementary Materials Figures S1–S3. These curves were the basis from which the tensile strength and the elongation at break data (Table 4), and tensile strength variation curves (Figures 3 and 4) were generated. The reduction in tensile strength was noticeable for the EPDM and silicone after 168 h of aging, and moderate for the FKM. In addition, the FKM and silicone showed different degrees of degradation, depending on the ATF used (Figure 3).

From 168 h onwards (long-term tensile strength behaviour), all the materials maintained relatively constant values of tensile strength, except for silicone in oil C. According to the limits established by the specifications used, the materials with compatibility problems are the EPDM and the silicone in oil C. In the case of the silicone, oils A, B, and D had a similar compatibility to that of the oil used by Farfan-Cabrera et al. [21], who reported just 2.5% tensile strength reduction when it was aged in synthetic oil at room temperature for 670 h. Kusuhara et al. [18] obtained similar values, but recognised that it could be degraded at relatively low temperatures due to the ionicity of Si-O bonds, causing compatibility problems with engine oils. This would correspond with the results with oil C, which shows a much more important reduction in the tensile strength.

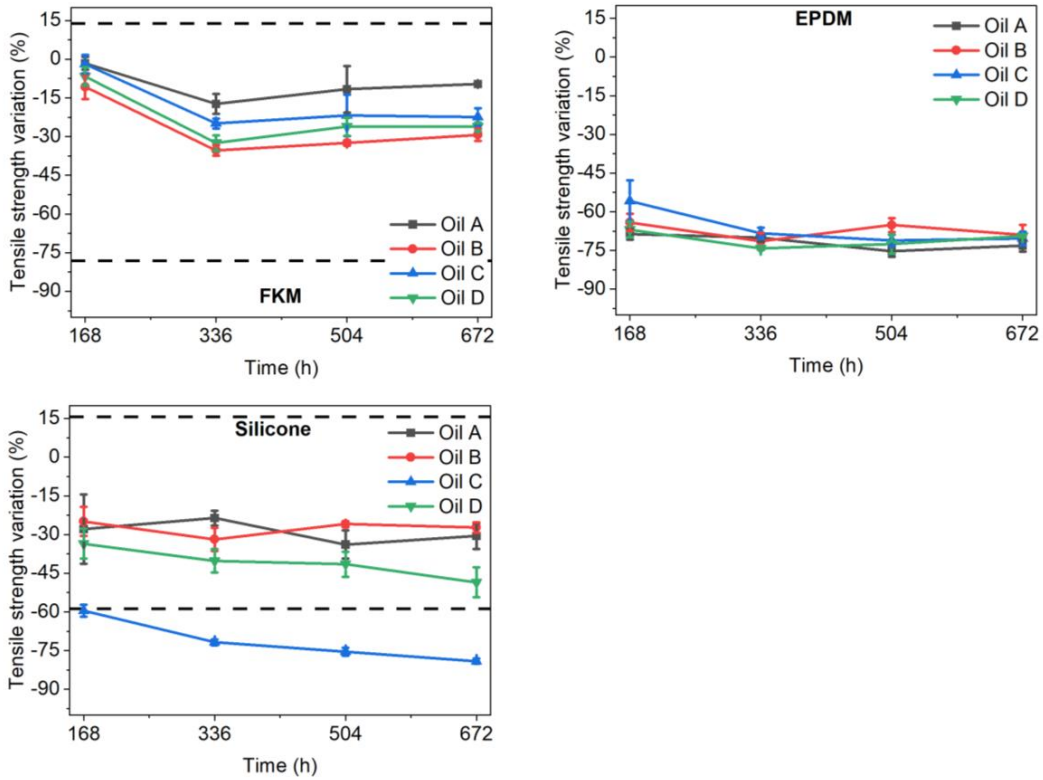

Figure 3. Changes in tensile strength (expressed as the ratio of the tensile strength variation to the initial tensile strength) of FKM, silicone, and EPDM after aging in oils A, B, C, and D.

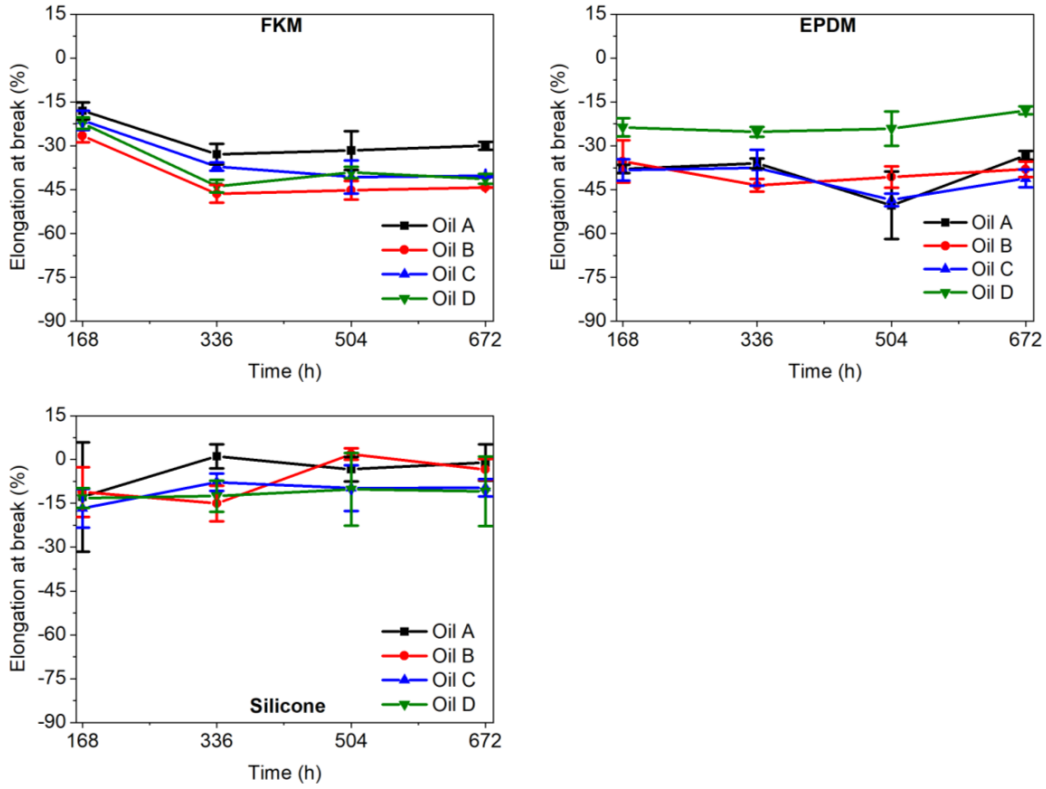

Figure 4. Changes in elongation at break (expressed as the ratio of the elongation at break variation to the initial elongation at break) of FKM, silicone, and EPDM, after aging in oils A, B, C, and D.

Regarding the elongation at break, all the elastomers showed similar behaviour, with a certain reduction in the measured values (Figure 4). Among these materials, the EPDM was the most affected by aging after 168 h (except in oil D), while the silicone showed the lowest reduction in this property, despite the higher variability of the measurements. After 168 h, the elongation at break was more affected by the aging process than the tensile strength was, except in the case of silicone (Figure 3), where there was also more variability in the results.

The elongation at break of the FKM followed a pattern similar to that of the tensile strength, which coincides with that reported by Tate et al. [23]. On the contrary, Zeng [13] reported a decrease of 50% in both the tensile strength and the elongation at break after 504 h, and no sign of stabilization was detected during the whole test. The results in the present study were similar to those reported by Zeng [13] up to 336 h, reaching a 45% decrease in the elongation at break with oil B, but remaining constant from that time until the end of the test.

The variation in the mechanical properties of the elastomers obtained in this research, even when, in some cases, they do not fulfil the transmission manufacturers specifications, are better than the results reported by Vaiden [24], Hull [25], Zeng and Dickerman [26], or Dobel and Bauerle [27]. This indicates the improvement of elastomeric technology that has taken place.

3.4. Results of Complementary Tests

The X-ray Diffraction (XRD) tests were used to look for changes in the crystalline structure of the materials. The level of crystallinity in a polymer reveals its long-range order and has an effect on its properties. The more crystalline a polymer is, the more regularly its chains are aligned. The density and hardness increase with the degree of crystallinity, which means that the calculation of the crystallinity of the polymers tested in this study was helpful in correlating and understanding the mechanical properties that were measured experimentally.

Considerable amounts of an amorphous substance in a phase mixture shows up as what is referred to as the amorphous profile. Instead of the characteristic diffraction peaks originated by a crystalline compound, X-rays are scattered continuously over a broad 2θ range. By defining the background intensity (separating the crystalline peaks from the amorphous profiles) and entering a constant background value, the HighScore software [28] calculates the crystallinity percentage automatically based on the following equation:

$$\text{Crystallinity [\%]} = 100 \times \Sigma I_{net.} / (\Sigma I_{tot.} - \Sigma\, I_{const.bgr.}) \quad (1)$$

where $I_{net.}$ represents the peak intensity (crystalline part), $I_{tot.}$ is the total intensity, and $I_{const.bgr.}$ is the intensity of the defined background (amorphous profile).

Figures 5–7 show the XRD spectra of the elastomers both in the fresh state and after 168 h of aging in each lubricant. The spectra of fresh and aged elastomers allow us to compare and identify possible changes in the structure of elastomers. Only the fresh and 168 h aged samples results are reported, as no influence of the aging time was found in the long term. Figures 5 and 6 show the same *y*-axis scale, while Figure 7 presents a larger *y*-axis scale due to the greater intensity of silicone peaks during the XRD analysis.

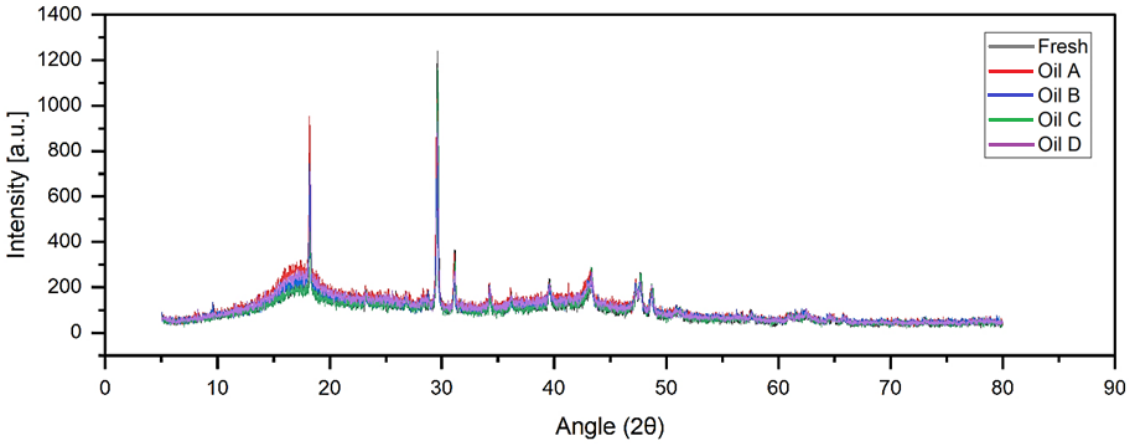

Figure 5. XRD spectra expressed in arbitrary units (a.u.) for the FKM (fresh and after 168 h of aging).

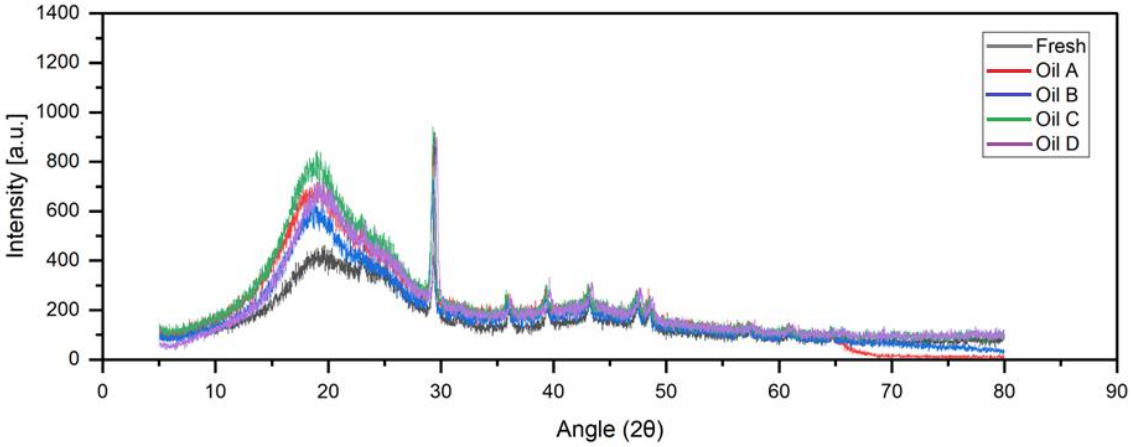

Figure 6. XRD spectra expressed in arbitrary units (a.u.) for the EPDM (fresh and after 168 h of aging).

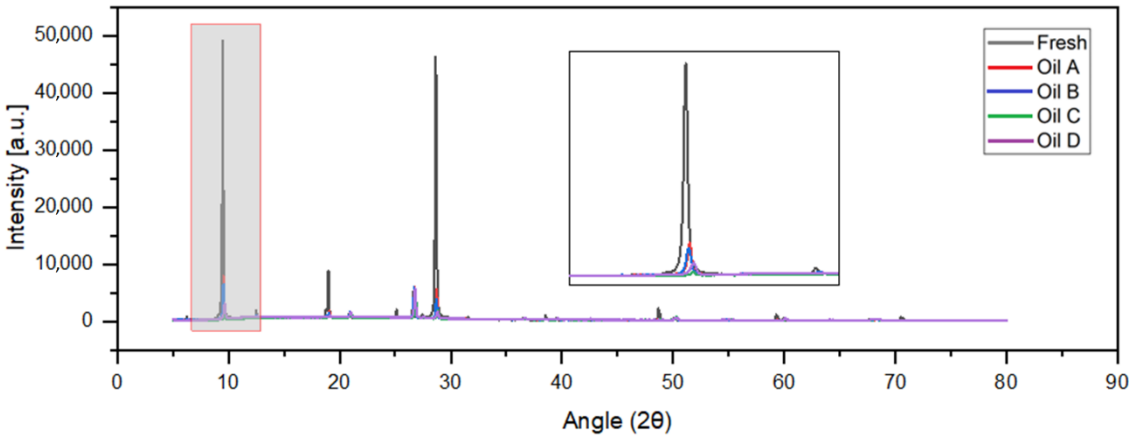

Figure 7. XRD spectra expressed in arbitrary units (a.u.) for the silicone (fresh and after 168 h of aging).

Table 5 shows the crystallinity percentage of FKM, according to Equation (1), after aging in the different lubricants for 168 and 672 h, as well as that of a fresh sample. It can be observed that the change in the crystallinity value with respect to the fresh sample was not significant (Table 5, Figure 5), which means that properties such as hardness and tensile strength would not change notably due to a variation in crystallinity. A qualitative analysis of the crystalline phases using the PDF4 database [29] integrated into the HighScore software found calcium carbonate ($CaCO_3$) and iron oxide (Fe_3O_4) as additives.

Table 5. Crystallinity percentage of the FKM samples for different aging times.

ATF	0 h	168 h	672 h
-	21.29	-	-
Oil A	-	13.47	13.50
Oil B	-	13.55	19.22
Oil C		20.33	18.64
Oil D	-	13.96	12.45

In the EPDM fresh sample, calcium carbonate was identified as a crystalline additive. However, it was not possible in this case to calculate the percentage of crystallinity accurately, because the profile observed between 6 and 28 2θ (Figure 6) did not allow separation of the amorphous area from the semi-crystalline area with a constant background methodology.

Table 6 shows the crystallinity percentage of silicone, according to Equation (1) after aging in the different lubricants for 168 and 672 h, as well as that of a fresh sample. The analysis of the crystallinity percentage values showed that the measured changes in mechanical properties (hardness and tensile strength) are indeed explained by the significant changes in the crystallinity percentage.

Table 6. Crystallinity percentage of the silicone samples for different aging times.

ATF	0 h	168 h	672 h
-	65.50	-	-
Oil A	-	26.20	34.76
Oil B	-	23.47	34.51
Oil C		18.73	17.35
Oil D	-	16.60	18.24

This decrease in crystallinity is well illustrated in the expanded window in Figure 7 and was reproduced in all of the crystalline phase peaks of the fresh silicone sample. Figure 7 had to be displayed with a different scale compared to Figures 5 and 6, as the crystallinity peaks are much sharper than in those cases, which is reflected in the crystallinity percentages of the respective fresh samples (65% for silicone, 21% for FKM, and unidentified for the EPDM). In addition, a qualitative analysis of the crystalline phases found silicon oxide (SiO_2) additive.

Figures 8–10 show the infrared absorbance spectra for samples of the elastomers: FKM, EPDM, and silicone, respectively. Results are shown for fresh material and after the aging process in different lubricants for 168 and 672 h. The FTIR tests were carried out to detect possible variations in the polymeric structure of the elastomers. The spectra of silicone (Figure 10) are reported as complete spectra (wavenumber between 600 to 4000 cm^{-1}) and an amplified section between 2750 and 3050 cm^{-1} in order to obtain a better understanding of the spectra peaks in this wavenumber interval.

The FKM spectra (Figure 8) show the characteristic bands for this polymer, which are summarised in Table S1 in the Supplementary Material. The area of every peak was compared between the different FKM samples and considered different when the area failed a Grubb's test ($p = 0.01$, $n = 9$). With this criterion, two main differences were found. First, the fresh sample showed a peak at 1735 cm^{-1} which became lower in the rest of the samples. This peak is assignable to the stretching vibrations of the $C{=}CF_2$ bond [30], which seems to be at least partially damaged after aging. Furthermore, the sample aged in oil A for 168 h showed significant reductions at 3020, 1390, and 1350 cm^{-1} which are assignable to asymmetric CH_2 stretching, $–CH_2–$ wagging vibration in $–CH_2F$, and C–F stretching in $C{=}CF_2$, respectively [30], suggesting partial damage. However, understanding why the peaks were present after 672 h needs further study. On the other hand, the fresh sample showed a very broad peak around 3275 cm^{-1}, which could be interpreted as indicating

the presence of water in the elastomer. This band was also present, although lower, in the sample with oil A after 168 h, but it disappeared in the rest of the samples, suggesting the elimination of retained water.

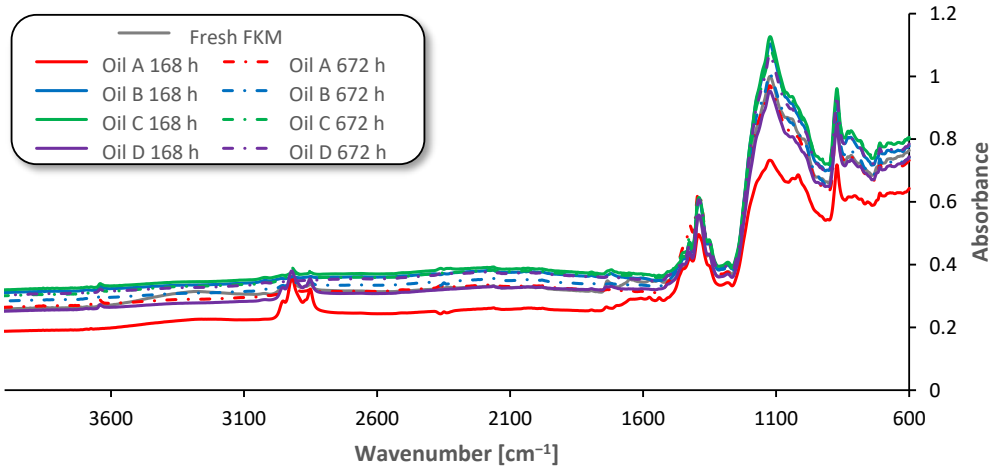

Figure 8. ATR-FTIR absorbance spectra (Beer's Law) of the FKM samples.

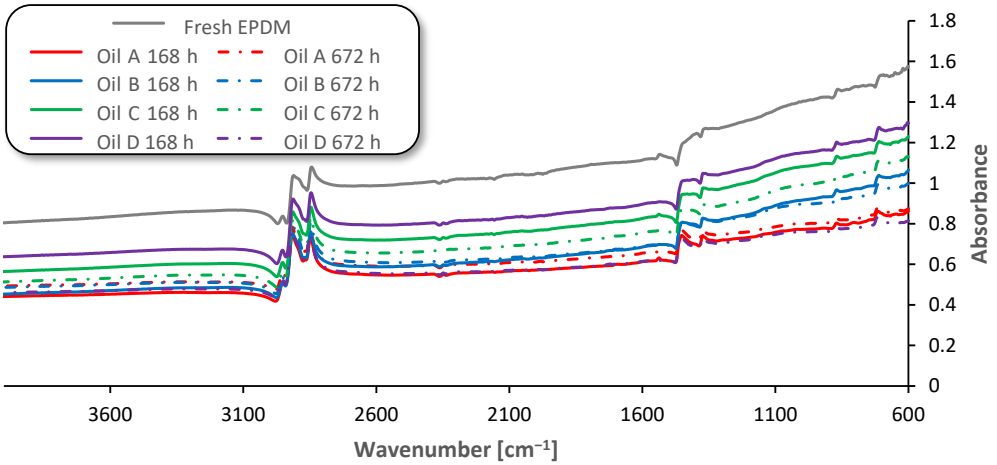

Figure 9. ATR-FTIR absorbance spectra (Beer's Law) of the EPDM samples.

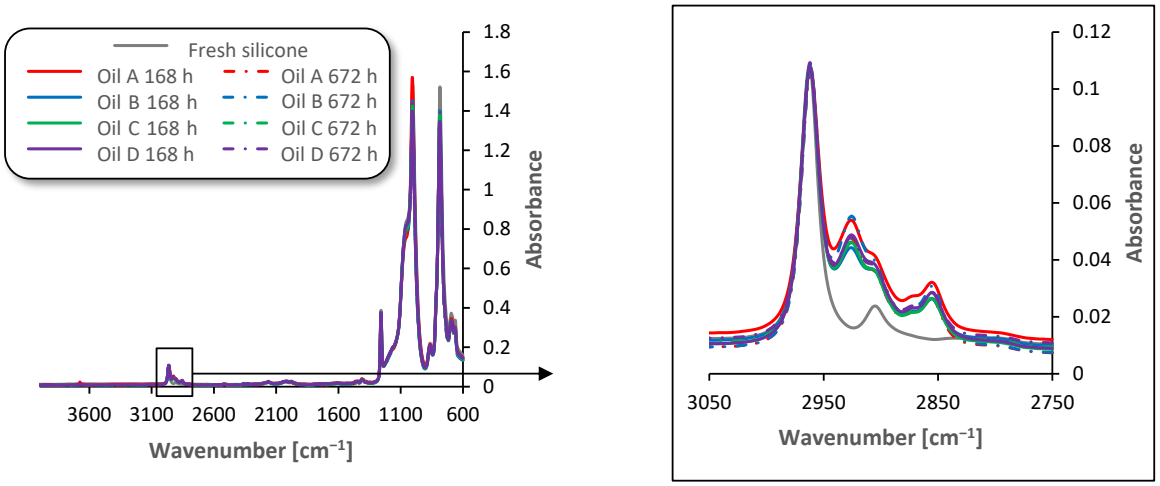

Figure 10. ATR-FTIR absorbance spectra (Beer's Law) of the silicone samples.

Regarding the EPDM samples, in addition to the bands at 2905 and 2840 cm^{-1}, assignable to –CH– stretching vibrations in alkanes [30], the band at 1450 cm^{-1} is also very apparent in Figure 8 and coincides with the strongest band in the FTIR spectrum of $CaCO_3$ [30]. Calcium carbonate is a common inorganic additive in polymers, and its presence has also been confirmed by XRD (Figure 6).

The different samples of silicone do not show significant differences in their basic structure. Thus, all samples maintain the characteristic Si–CH_3 peaks at 784 and 865 cm^{-1} (stretching vibration) and 1257 cm^{-1} (rocking vibration), as well as a broad band at 1004 cm^{-1} that corresponds to the Si–O–Si asymmetric stretching. The band at 1411 cm^{-1} reveals the presence of Si–$CH{=}CH_2$ in all the samples, too [31]. Likewise, two bands at 2890 and 2960 cm^{-1}, corresponding to the CH_3 symmetric and asymmetric stretching vibrations, respectively, are also present [30]. However, after coming into contact with each oil, and regardless of the contact time, VMQ samples showed two new bands at 2855 cm^{-1} and 2925 cm^{-1}, which are very likely from –CH_2– symmetric and asymmetric stretching vibrations, respectively (Figure 10) [30]. This result indicates the presence of new hydrocarbon chains in the material, which appeared after contact with the oil. This suggests the incorporation of the oil into the silicone material, which is reasonable, bearing in mind the increase in volume shown in Figure 1.

Figures 11–13 show the thermogravimetric analysis for samples after aging for 168 h of FKM, EPDM, and silicone, respectively. Each figure shows both the percentage loss in weight with respect to the temperature (TGA), as well as the derivative of the aforementioned loss with time (DTGA). The thermogravimetic analysis allows us to analyse how the aging process could affect the structure of the elastomers and their thermal stability. Tables 7–9 show the detailed values of the thermogravimetric analysis for each material. Only the fresh and 168 h aged samples results are reported, as no influence of the aging time was found in the long term.

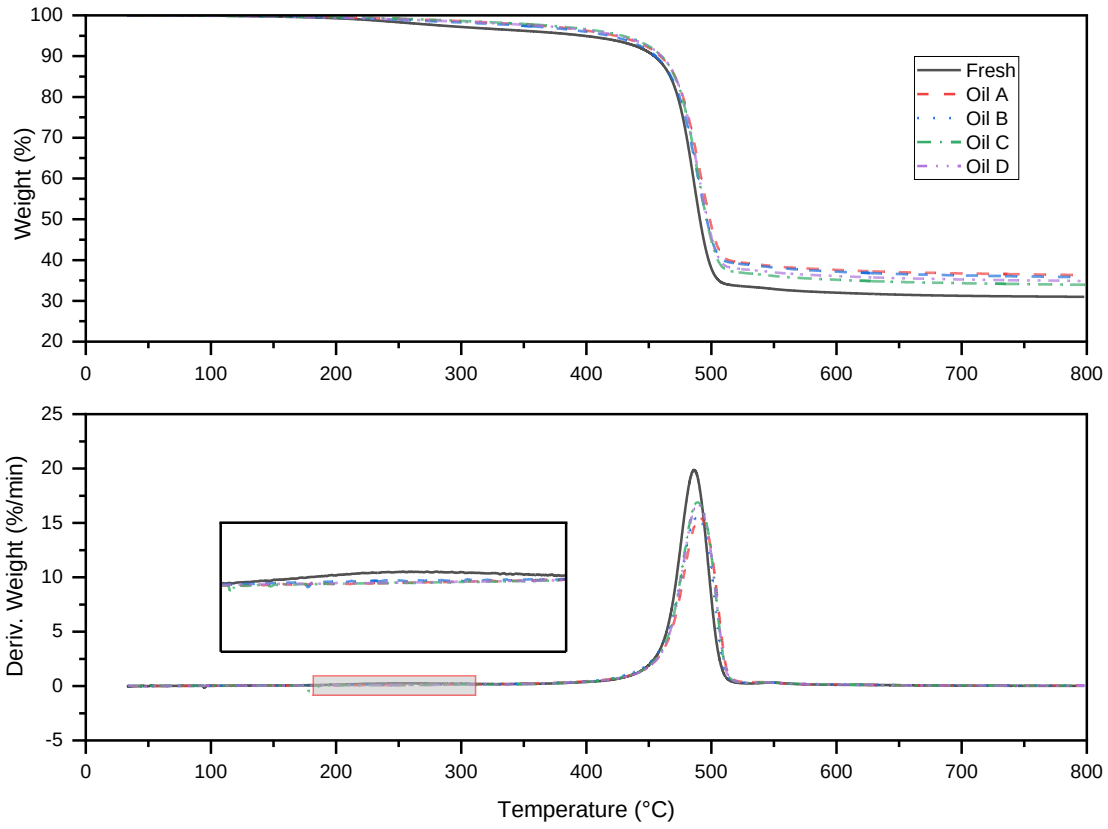

Figure 11. TGA (above) and DTGA (below) curves expressed as mass percentage and mass percentage over time, for fresh and 168 h aged FKM.

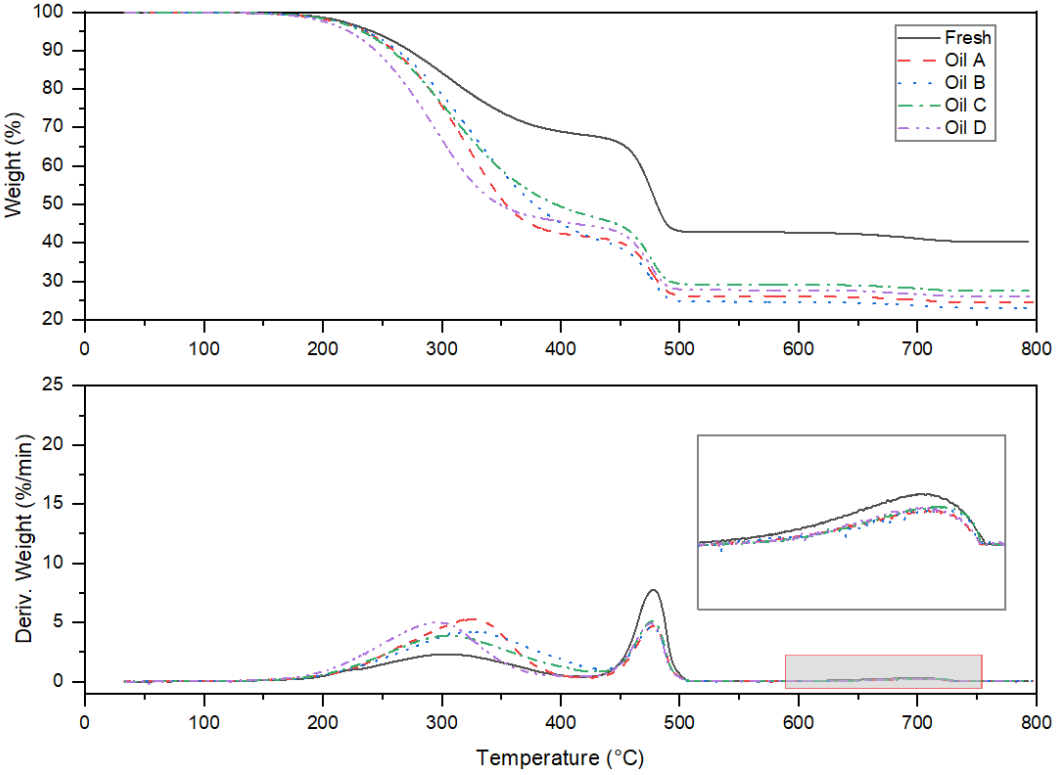

Figure 12. TGA (above) and DTGA (below) curves expressed as mass percentage and mass percentage over time, for fresh and 168 h aged EPDM.

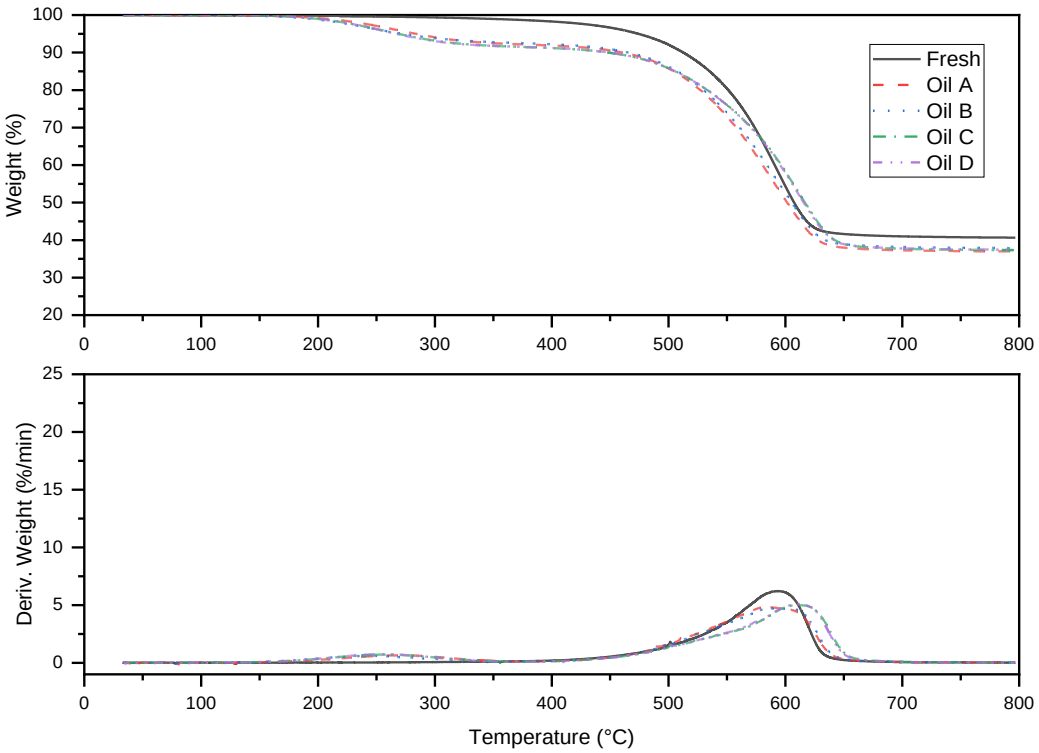

Figure 13. TGA (above) and DTGA (below) curves expressed as mass percentage and mass percentage over time, for fresh and 168 h aged silicone.

Table 7. TGA and DTGA data of fresh and 168 h aged FKM.

ATF	T_{onset} [°C]	T_{endset} [°C]	WL_{Total} [%]	T_{peak} [°C]
Fresh	468	499	69.0	486
Oil A	468	503	66.9	489
Oil B	465	503	64.2	488
Oil C	468	504	65.7	489
Oil D	468	504	64.9	489

Table 8. TGA and DTGA data for fresh and 168 h aged EPDM.

ATF	Step 1				Step 2				Step 3			
	T_{onset} [°C]	T_{endset} [°C]	WL [%]	T_{peak} [°C]	T_{onset} [°C]	T_{endset} [°C]	WL [%]	T_{peak} [°C]	T_{onset} [°C]	T_{endset} [°C]	WL [%]	T_{peak} [°C]
Fresh	236	360	31.5	303	459	489	25.5	478	635	722	2.4	707
Oil A	245	363	57.7	325	458	490	16.2	477	643	723	1.5	705
Oil B	248	378	58.5	330	458	489	16.5	477	674	725	1.4	716
Oil C	240	363	53.1	362	460	489	18.0	475	662	726	1.6	710
Oil D	234	337	54.7	297	456	489	17.6	476	660	721	1.6	704

Table 9. TGA and DTGA data of fresh and 168 h aged silicone.

ATF	Step 1				Step 2			
	T_{onset} (°C)	T_{endset} (°C)	WL (%)	T_{peak} (°C)	T_{onset} (°C)	T_{endset} (°C)	WL (%)	T_{peak} (°C)
Fresh	-	-	-	-	512	621	59.3	592
Oil A	212	314	7.6	271	502	626	55.2	584
Oil B	195	298	7.1	246	500	629	54.8	587
Oil C	205	306	8.2	257	508	640	54.3	612
Oil D	199	301	8.5	257	517	639	54.0	611

The mechanism of degradation of FKM by dehydrofluorination and chain scission is discussed in previous papers [32]. The major degradation starts at 468 °C (T_{onset}) and is completed at 503 °C (T_{endset}), as can be observed in Figure 11 and Table 7. These results are in good agreement with the literature [33,34]. No noteworthy event was observed at temperatures above the T_{endset}. Below, the T_{onset} the loss of mass is about 4% and might be due to the presence of volatile matter in the composition (evaporation of some small organic molecules and other additives used in the fabrication of the rubber and the oils). For the aged samples, the TGA curves follow the same trend (Figure 11). However, the loss of weight is slightly lower (Table 7), especially at low temperatures (below T_{onset}). This difference can be explained by the loss of the volatile components of the elastomer during the heat-aging process, which is consistent with their volume reduction (Figure 1).

The thermal degradation process of the EPDM is more complex, as can be seen in Figure 12. The TG curve shows a three-stage mass loss process, and the DTG curve shows the three corresponding peaks at 303, 478, and 707 °C. The first stage occurred between 236 and 360 °C and was due to the loss of volatile matter present in the composition of the elastomer [35] and it constituted the main mass degradation (31.5%). The next stage occurred over the 458–490 °C range, with a 25.52% weight reduction due to the elastomeric matrix degradation. This second stage of thermal decomposition is attributed to the scission of cross-linked EPDM with elimination of carbon dioxide, water, carbon monoxide, methane, and ethane [36]. Finally, the third stage occurred within the 635 to 722 °C temperature range, with the loss of 2.4% of the initial weight, corresponding to the decomposition of the calcium carbonate additive, whose presence was confirmed by XRD and FTIR. The residual mass was around 40%, which would be composed of mineral components. For aged samples, the TGA curves followed the same trend. However, the weight reduction during the first stage was much greater (Table 8) due to the loss of the

different oils that had previously been absorbed into the rubber matrix. This absorption process would be related to the changes observed in the measured mechanical properties, such as the huge increase in volume (Figure 1) and the equally large hardness reduction (Figure 2).

Finally, the TGA curve of the fresh silicone revealed a higher thermal stability (Figure 13). The only stage of degradation for this sample occurred between 468 and 503 °C with a DTG peak at 526 °C. The volatile fraction is negligible, so the total loss of weight can be ascribed to polymeric decomposition. In this case, the aging process induced some changes in the shape of the thermogravimetric curves. It is shown in Figure 13 how, unlike the fresh polymer, which only had one decomposition step, two stages appear after aging in all the ATFs. The first stage, starting at temperatures close to 200 °C (Table 9), is due to the evaporation of the oil medium that was dispersed in the silicone, similarly to what happened in EPDM. Due to this adsorption process, the total loss of weight increased and, thus, the degree of crystallinity decreased, as the total weight was increased by oil, which has null crystallinity. The second weight reduction corresponded to polymeric thermal degradation.

Table 10 shows a summary chart of the compatibility between the different elastomers and lubricants made by the authors based on the set of tests carried out and discussed above. With respect to the variations in the mechanical properties tested for the aged elastomers, the four oils would be compatible with silicone as regards volume variation, while none of them would permit the specifications for FKM and EPDM to be achieved. In the case of hardness change, the four oils are compatible with FKM and silicone, while EPDM has the highest decline in this property among all the elastomers. Although there is no specification provided by the transmissions manufacturers for this material, Nakamura et al. [19] suggested that seals made of EPDM with a lower loss of hardness would break into small pieces, so EPDM would not be compatible with these oils. Regarding the resistance properties (tensile strength and elongation at break) variation, the four oils would be compatible with FKM, and only oil C would be incompatible with silicone. Again, EPDM shows the biggest decline in these properties with all the oils, with similar values to those of oil C with silicone, which indicates that the oils in the trial are not compatible with this material. These results allow the degree of compatibility between the ATFs and the elastomers to be established, as shown in Table 10.

Table 10. Oil compatibility with the studied elastomers.

ATF	FKM	EPDM	Silicone
Oil A	**	*	***
Oil B	**	*	***
Oil C	**	*	**
Oil D	**	*	***

* Low compatibility; ** Medium compatibility; and *** High compatibility.

4. Conclusions

Four different ATFs were tested to check their compatibility with three elastomeric materials commonly used as seals and gaskets in the transmissions of electric vehicles, as well as for the insulation of electric wiring. These materials were tested according to the recommendations of transmissions manufacturers regarding the admissible changes in hardness, volume, and resistance properties after aging these materials in ATFs. The variations found in the mechanical properties could have been related to variations in the composition and crystalline structure of the elastomers, and therefore some complementary tests (FT-IR, XRD, and TGA) were performed to clarify the results. This research allows the readers to infer that the lubricant composition and the type of seal and gasket materials are important in terms of compatibility. This research has been conducted with three standard materials used in seals, and then, general conclusions are deduced for each combination of lubricant and material. A more detailed compatibility study for a specific EV would

require a detailed test of the specific lubricant and materials for each application, using the same methodology proposed in this manuscript. From the results, we can conclude that:

- The four ATFs caused similar effects on each material, except for oil C and oil A, which reduced the tensile strength of the silicone and increased the volume of the EPDM, respectively, making them incompatible.
- A significant reduction in the crystalline structure of the silicone was indicated by the XRD tests, this reduction being higher after aging in oil C, which led to this combination not fulfilling the specifications regarding tensile strength. The crystalline structure variation in FKM was not important, and it was not possible to make the calculations for the EPDM due to its semi-crystalline nature.
- The FT-IR tests helped to confirm the presence of the oils inside the structure of the aged silicone samples, which would have contributed to the swelling and softening of the material.
- Due to oil absorption in the polymeric matrix, chemical and structural changes were detected in the EPDM and silicone, causing a volume increase which led to reductions in hardness and tensile strength. The FKM did not absorb any oil during the aging process, but the evaporation of the volatile components present in the fresh rubber caused a decrease in the volume and an increase in hardness.
- The non-compatibility of the EPDM with the oils from Group III was also proven.
- The compatibility of these ATFs with some of the elastomers tested is an essential requirement but is not sufficient without further trials involving other properties. More compatibility tests (magnetic, electrical, corrosion, thermal, foaming at high speeds, and aeration) should be conducted on the ATFs before using them in an electrified transmission.

Supplementary Materials: The following supporting information can be downloaded at: https://www.mdpi.com/article/10.3390/app12126213/s1, Figure S1. Tensile strength and elongation at break for FKM and oils A to D (Fresh and after aging periods of 168, 336, 504 and 672 h); Figure S2. Tensile strength and elongation at break for EPDM and oils A to D (Fresh and after aging periods of 168, 336, 504 and 672 h); Figure S3. Tensile strength and elongation at break for Silicone and oils A to D (Fresh and after aging periods of 168, 336, 504 and 672 h); Table S1. Characteristic FTIR spectra bands for FKM. References [37,38] are cited in the supplementary materials.

Author Contributions: Conceptualization, A.G. and A.H.B.; Methodology, A.G., A.G.-T. and A.F.-G.; Investigation, A.G., G.D.V., B.R. and R.M.; Writing—original draft, A.G., A.G.-T. and A.F.-G.; Supervision, A.H.B.; Project administration, A.H.B.; Writing—review and editing, A.H.B. All authors have read and agreed to the published version of the manuscript.

Funding: This research was funded by Ministry of Science, Innovation and Universities (Spain), grant number PID2019-109367RB-I00.

Institutional Review Board Statement: Not applicable.

Informed Consent Statement: Not applicable.

Data Availability Statement: Data is contained within the article or Supplementary Materials.

Acknowledgments: The authors would like to acknowledge the Ministry of Science, Innovation and Universities (Spain) for supporting this work under the project PID2019-109367RB-100 and the technical support provided by Scientific and Technical Services of the University of Oviedo.

Conflicts of Interest: The authors declare no conflict of interest.

References

1. Intergovernmental Panel on Climate Change. *Climate Change 2014 Mitigation of Climate Change*; Cambridge University Press: Cambridge, UK, 2014; ISBN 9781107654815.
2. Holmberg, K.; Erdemir, A. The Impact of Tribology on Energy Use and CO_2 Emission Globally and in Combustion Engine and Electric Cars. *Tribol. Int.* **2019**, *135*, 389–396. [CrossRef]
3. Woydt, M. The Importance of Tribology for Reducing CO2 Emissions and for Sustainability. *Wear* **2021**, *474–475*, 203768. [CrossRef]

4. Bellekom, S.; Benders, R.; Pelgröm, S.; Moll, H. Electric Cars and Wind Energy: Two Problems, One Solution? A Study to Combine Wind Energy and Electric Cars in 2020 in The Netherlands. *Energy* **2012**, *45*, 859–866. [CrossRef]
5. Xue, Q.; Zhang, X.; Teng, T.; Zhang, J.; Feng, Z.; Lv, Q. A Comprehensive Review on Classification, Energy Management Strategy, and Control Algorithm for Hybrid Electric Vehicles. *Energies* **2020**, *13*, 5355. [CrossRef]
6. Farfan-Cabrera, L.I. Tribology of Electric Vehicles: A Review of Critical Components, Current State and Future Improvement Trends. *Tribol. Int.* **2019**, *138*, 473–486. [CrossRef]
7. García, A.; Valbuena, G.D.; García-Tuero, A.; Fernández-González, A.; Viesca, J.L.; Battez, A.H. Compatibility of Automatic Transmission Fluids with Structural Polymers Used in Electrified Transmissions. *Appl. Sci.* **2022**, *12*, 3608. [CrossRef]
8. Rodríguez, E.; Rivera, N.; Fernández-González, A.; Pérez, T.; González, R.; Battez, A.H. Electrical Compatibility of Transmission Fluids in Electric Vehicles. *Tribol. Int.* **2022**, *171*, 107544. [CrossRef]
9. Technical Team of Afton Chemical Company. *Afton Specification Handbook*; Afton Chemical: Richmond, VA, USA, 2019.
10. Braun, J. Current Elastomer Compatibility Test Standards—A Critical View. *Seal. Technol.* **2011**, *2011*, 8–12. [CrossRef]
11. Du, B.X.; Kong, X.X.; Li, J.; Xiao, M. High Thermal Conductivity Insulation and Sheathing Materials for Electric Vehicle Cable Application. *IEEE Trans. Dielectr. Electr. Insul.* **2019**, *26*, 1363–1370. [CrossRef]
12. Bulut, D.; Krups, T.; Poll, G.; Giese, U. Lubricant Compatibility of FKM Seals in Synthetic Oils. *Ind. Lubr. Tribol.* **2020**, *72*, 557–565. [CrossRef]
13. Zeng, N. Compatibility Study of Fluorinated Elastomers in Automatic Transmission Fluids. In Proceedings of the 2008 SAE International Powertrains, Fuels and Lubricants Congress, Hong Kong, China, 24 June 2008; SAE International: Warrendale, PA, USA, 2008.
14. *ASTM D7216-15*; Standard Test Method for Determining Automotive Engine Oil Compatibility with Typical Seal Elastomers. ASTM International: West Conshohocken, PA, USA, 2015.
15. Haghshenas, N.; Nejat, A.; Seyedmehdi, S.A.; Ou, J.; Amirfazli, A.; Chini, S.F. Adhesion Aspects of Silicone Rubber Coatings for High Voltage Insulators: A Critical Review. *Rev. Adhes. Adhes.* **2021**, *9*, 434. [CrossRef]
16. Flitney, R. *Seals and Sealing Handbook: Sixth Edition*; Elsevier Inc.: Amsterdam, The Netherlands, 2014; ISBN 9780080994161.
17. Drobny, J.G. Compounds for Automotive Power Train Systems. In *Fluoroelastomers Handbook*; Elsevier: Amsterdam, The Netherlands, 2016; pp. 483–490.
18. Kusuhara, S.; Yoshimura, K.; Kunieda, K.; Suzuki, N.; Matsuki, S.; Shitara, Y. Experimental Investigation on the Influence of Engine Oil Additives on Silicone Rubber. *SAE Int. J. Fuels Lubr.* **2017**, *10*, 461–468. [CrossRef]
19. Nakamura, T.; Chaikumpollert, O.; Yamamoto, Y.; Ohtake, Y.; Kawahara, S. Degradation of EPDM Seal Used for Water Supplying System. *Polym. Degrad. Stab.* **2011**, *96*, 1236–1241. [CrossRef]
20. de Souza, E.L.; de Souza Zanzi, M.; de Paiva, K.V.; Goes Oliveira, J.L.; Monteiro, A.S.; de Oliveira Barra, G.M.; Dutra, G.B. Evaluation of the Aging of Elastomeric Acrylonitrile-Butadiene Rubber and Ethylene-Propylene-Diene Monomer Gaskets Used to Seal Plates Heat Exchanger. *Polym. Eng. Sci.* **2021**, *61*, 3001–3016. [CrossRef]
21. Farfán-Cabrera, L.I.; Gallardo-Hernández, E.A.; Reséndiz-Calderón, C.D.; Sedano de la Rosa, C. Physical and Tribological Properties Degradation of Silicone Rubber Using Jatropha Biolubricant. *Tribol. Trans.* **2018**, *61*, 640–647. [CrossRef]
22. Petit, J.; Fewkes, R.; O'Brien, C. Seal Testing in Aerated Lubricants. In Proceedings of the SAE 2011 World Congress and Exhibition, Detroit, MI, USA, 12 April 2011.
23. Tate, N.; Saito, M.; Sugitani, K. Fluoroelastomer Resistant to Automotive Lubricants. In *SAE Technical Papers*; SAE International: Warrendale, PA, USA, 2003.
24. Vaiden, R.E. Elastomeric Materials for Engine and Transmission Gaskets. In *SAE Technical Papers*; SAE International: Warrendale, PA, USA, 1992. [CrossRef]
25. Hull, D.E.; Eggers, R.E.; Horemans, E. *New Elastomers Are More Resistant to Many Automotive Fluids*; SAE Technical Paper 890361; SAE: Detroit, MI, USA, 1989.
26. Zeng, N.; Dickerman, R.L. Development of Additional SAE J2643 Standard Reference Elastomers. *SAE Int. J. Mater. Manuf.* **2011**, *4*, 40–74. [CrossRef]
27. Dobel, T.M.; Bauerle, J.G. New FKM Developments for Automotive Powertrain Applications. In *SAE Technical Papers*; SAE International: Warrendale, PA, USA, 2000; pp. 263–269. [CrossRef]
28. Degen, T.; Sadki, M.; Bron, E.; König, U.; Nénert, G. The HighScore Suite. *Powder Diffr.* **2014**, *29*, S13–S18. [CrossRef]
29. Gates-Rector, S.; Blanton, T. The Powder Diffraction File: A Quality Materials Characterization Database. *Powder Diffr.* **2019**, *34*, 352–360. [CrossRef]
30. Socrates, G. Infrared and Raman Characteristic Group Frequencies. In *Tables and Charts*; John Wiley & Sons: Hoboken, NJ, USA, 2001; ISBN 978-0-470-09307-8.
31. Shivakumar, E.; Das, C.K.; Pandey, K.N.; Alam, S.; Mathur, G.N. Blends of Silicone Rubber and Liquid Crystalline Polymer. *Macromol. Res.* **2005**, *13*, 81–87. [CrossRef]
32. Sugama, T.; Pyatina, T.; Redline, E.; McElhanon, J.; Blankenship, D. Degradation of Different Elastomeric Polymers in Simulated Geothermal Environments at 300 °C. *Polym. Degrad. Stab.* **2015**, *120*, 328–339. [CrossRef]
33. Kader, M.A.; Lyu, M.Y.; Nah, C. A Study on Melt Processing and Thermal Properties of Fluoroelastomer Nanocomposites. *Compos. Sci. Technol.* **2006**, *66*, 1431–1443. [CrossRef]

34. Singh, A.; Soni, P.K.; Sarkar, C.; Mukherjee, N. Thermal Reactivity of Aluminized Polymer-Bonded Explosives Based on Non-Isothermal Thermogravimetry and Calorimetry Measurements. *J. Therm. Anal. Calorim.* **2019**, *136*, 1021–1035. [CrossRef]
35. Rojas Rodríguez, F.I.; D'almeida, J.R.M.; Marinkovic, B.A. Natural Aging of Ethylene-Propylene-Diene Rubber under Actual Operation Conditions of Electrical Submersible Pump Cables. *Materials* **2021**, *14*, 5520. [CrossRef] [PubMed]
36. Bouguedad, D.; Mekhaldi, A.; Jbara, O.; Rondot, S.; Hadjadj, A.; Douglade, J.; Dony, P. Physico-Chemical Study of Thermally Aged EPDM Used in Power Cables Insulation. *IEEE Trans. Dielectr. Electr. Insul.* **2015**, *22*, 3207–3215. [CrossRef]
37. Kang, H.; Chen, L.; Du, H.; Wang, H.; Li, D.; Fang, Q. Hot Nitric Acid Diffusion in Fluoroelastomer Composite and Its Degradation. *RSC Adv.* **2019**, *9*, 38105–38113. [CrossRef]
38. Mitra, S.; Ghanbari-Siahkali, A.; Kingshott, P.; Almdal, K.; Rehmeier, H.K.; Christensen, A.G. Chemical Degradation of Fluoroelastomer in an Alkaline Environment. *Polym. Degrad. Stab.* **2004**, *83*, 195–206. [CrossRef]